Learning to discriminate between ligand bound and disulfide bound cysteines

Andrea Passerini[1] **and Paolo Frasconi**

Dipartimento di Sistemi e Informatica
Università di Firenze
50139 Firenze, Italy

[1]Corresponding author. E-mail: passerini@dsi.unifi.it

Running title
Cysteine binding type prediction

Abstract

We present a machine learning method to discriminate between cysteines involved in ligand bindings and cysteines forming disulfide bridges. Our method uses a window of multiple alignment profiles to represent each instance and support vector machines with polynomial kernel as learning algorithm. We also report results obtained with two new kernel functions based on similarity matrices. Experimental results indicate that binding type can be predicted at significantly higher accuracy than using PROSITE patterns.

keywords. Disulfide bridges/metal binding sites/prediction tools/support vector machines.

1 Introduction

Non-free cysteines that are not involved in the formation of disulfide bridges usually bind prosthetic groups that include a metal ion and that play an important role in the function of a protein. The discrimination between the presence of a disulfide bridge (DB) or a metal binding site (MBS) in correspondence of a bound cysteine is often a necessary step during the NMR structural determination process of metalloproteins, and its automation may significantly help towards speeding up the overall process. Several proteins are known where both situations are in principle plausible and it is not always possible to assign a precise function to each cysteine. For example the mitochondrial copper metallochaperone Cox17 contains six cysteines but it is not precisely known which ones are actually involved in metal binding (Heaton et al., 2001). Another example is the inner mitochondrial membrane protein sco1p that contains a CxxxC motif and experimental evidence that could lead us to believe it is involved in copper transport, but whose fold similarity to a thioredoxin fold could conversely suggest a catalytic activity (Chinenov, 2000; Balatri et al., 2003).

In addition to the above motivations, the discrimination between DBs and MBSs may help towards a more accurate prediction of the disulfide bonding state of cysteines (Fiser and Simon, 2000). In this task, global descriptors (Mucchielli-Giorgi et al., 2002) and global postprocessing (Martelli et al., 2002) can help to predict the overall tendency of a chain to form or not to form bridges. However, current prediction methods typically fail to identify the type of binding in which each single bound cysteine is involved.

In some well known cases, the presence of a binding site for a prosthetic groups can be detected by inspecting the consensus pattern that matches the portion of the protein sequence containing the target cysteine. For example the 4Fe-4S ferredoxin group is associated with the pattern `C-x(2)-C-x(2)-C-(x3)-C-[PEG]` (Otaka and Ooi, 1987). Using annotated chains from Swiss-Prot and PDB we show that a set rules based on PROSITE (Falquet et al., 2002) patterns can be actually used to separate MBSs from DBs. Many of these rules are highly specific but there are well known examples of false positives. For example, the `C-{CPWHF}-{CPWR}-C-H-{CFYW}` consensus pattern is often correctly associated with a cytochrome c family heme binding site (Mathews, 1985), but the precision of such pattern is less than 40%. In addition, there are cases of cysteines involved in a MBS and having no associated pattern.

In this paper we formulate the prediction task as a binary classification problem: given a non-free cysteine and information about flanking residues, predict whether the cysteine can bind to a prosthetic group containing a metal ion (positive class) or it is always bound to another cysteine forming a disulfide bridge (negative class).

Firstly, we suggest a nontrivial baseline predictor based on PROSITE pattern hits and the induction of decision trees using the program C4.5 (Quinlan, 1993). Secondly, we introduce a classifier fed by multiple alignment profiles and based on support vector machines (SVM) (Cortes and Vapnik, 1995). We show that the latter classifier is capable of discovering the large majority of the relevant PROSITE patterns, but is also sensitive to signal in the profile sequence that cannot be detected by regular expressions and therefore outperforms the baseline predictor.

2 Materials and methods

2.1 Data preparation

The data for cysteines involved in disulfide bridge formation was extracted from PDB (Berman et al., 2000),We excluded chains if:

- the protein was shorter than 30 residues;
- it had less than two cysteines;
- it had cysteines marked as unresolved residues in the PDB file;

The data for metal binding sites was extracted from SWISS-PROT version 41.23 (Boeckmann et al., 2003), since PDB does not contain enough examples of metal ligands. In this case we included all entries containing at least one cysteine involved in a metal binding, regardless of the annotation confidence.

In this way examples of bindings with iron-sulfur clusters (2FE2S,3FE4S,4FE4S), copper, heme groups, iron, manganese, mercury, nickel and zinc were obtained.

Intra-set redundancy due to sequence similarity was avoided by running the UniqueProt program (Mika and Rost, 2003) with hssp distance set to zero. Inter-set redundancy however was kept in order to handle proteins with both disulfide bridges and metal bindings. It must be remarked that while inter-set redundancy can help the learning algorithm by providing additional data for training, it cannot favorably bias accuracy estimation since redundant cases should be assigned to opposite classes. The number of non-homologous sequences remaining in the datasets are shown in table 1 , together with the number of cysteines involved in bridges or metal bindings. Free cysteines were ignored.

2.2 PROSITE patterns as a baseline

In this section we establish a procedure to compute a baseline accuracy for the prediction task studied in this paper. In general, the base accuracy of a binary classifier is the frequency of the most common class. For the data set described above the base accuracy is 84.4%. In total absence of prior knowledge a predictor that performs better than the base accuracy is generally considered as successful. However:

- it must be remarked that, especially for highly unbalanced datasets, precision/recall rates are also needed in order to have a correct view of the classifier performance.
- for the task studied in this paper several well known consensus patterns exist that are associated with disulfide bridges and with metal binding sites. These patterns partially encode expert knowledge and it seems reasonable, when possible, to make use of them as a rudimentary prediction tool.

Thus, in order to compare our prediction method with respect to a more interesting baseline than the mere base accuracy, we extracted features that consist of PROSITE (Falquet et al., 2002) pattern hits.

A PROSITE pattern is an annotated regular expression that describes a relatively short portion of a protein sequence that has a biological meaning. We run the program `ScanProsite` (Gattiker et al., 2002) on the data set described above searching for patterns listed in the release 18.18 (December 2003) of PROSITE. In this way we found 199 patterns whose matches with the sequences in our data set contain the position of at least one bound cysteine. About 56% of the cysteines bound to a metal ion and about 41% of the cysteines forming disulfide bridges matched at least one PROSITE pattern. Many of the patterns associated with DBs have perfect (100%) specificity but each one only covers a very small set of cases. Overall, the fraction of disulfide-bond cysteines matched by a perfectly specific pattern is about 26%. Patterns associated with MBSs have a significantly higher coverage, although their specificity is perfect only about 18% of the times and sometimes is low. We remark that in our context a metal binding pattern is perfectly specific if every match is actually a metal binding site, regardless of the metal involved in the bond. Thus, examples of perfectly specific patterns associated with MBSs include PS00198 (4Fe-4S ferredoxins iron-sulfur binding region), PS00190 (Cytochrome c family heme-binding site), and PS00463 (Fungal Zn(2)-Cys(6) binuclear cluster domain). To further complicate the scenario, 12% of the bound cysteines match more than one pattern. For these reasons, a prediction rule based on pattern matches is difficult to craft by hand and we used the program C4.5 to create rules automatically from data. C4.5 induces a decision trees from labeled examples by recursively partitioning the instance space, using a greedy heuristic driven by information theoretic considerations (Quinlan, 1986). Rules are then obtained by visiting the tree from the root to a leaf. When using C4.5, each bound cysteine was simply represented by the bag of its matching patterns.

2.3 Support vector machines algorithm

Support vector machines (SVM) have been introduced in (Cortes and Vapnik, 1995) and give a well-posed formulation to the supervised learning problem so that a unique solution can be obtained once certain entities have been fixed. Here we briefly sketch the main ideas and notation of the general algorithm to allow proper replication of our experiments. Details can be found in several textbooks including (Cristianini and Shawe-Taylor, 2000; Schölkopf and Smola, 2002).

Training data is a set of pairs $D_m = \{(\boldsymbol{x}_i, y_i)\}_{i=1}^m$ where $\boldsymbol{x}_i$ is the input (in our case a real vector of features describing the context around a target cysteine) and y_i is the output class, either $+1$ (indicating a metal-ion binding) or -1 (indicating a disulfide bridge). The algorithm learns from the data a classification function f that can be used to make predictions about new instances. This function can be written as:

$$f(\boldsymbol{x}) = \sum_{i=1}^{m} y_i \alpha_i K(\boldsymbol{x}, \boldsymbol{x}_i) + \beta_0 \tag{1}$$

where $\alpha_1, \ldots, \alpha_m, \beta_0$ are parameters adjusted by the learning procedure and K is the *kernel*, a *positive semidefinite symmetric* function that measures the similarity between two input vectors and that can be thought of as a generalized dot product. The solution is a minimizer of the following functional:

$$H(f) = \sum_{i=1}^{m} \frac{C}{m} |1 - y_i f(\boldsymbol{x}_i)|_+ + \frac{1}{2}\|f\|_K^2 \tag{2}$$

where $|a|_+ = a$ if $a > 0$ and zero otherwise, and $\|f\|_K^2$ is the norm of the classification function f induced by the kernel K. The above functional is the sum of two terms: the leftmost one penalizes solutions that do not classify correctly (and with large margin) training data, while the rightmost one is a *regularizer* that penalizes too complex solutions and allows us to avoid overfitting. The quantity C expresses the relative weight of the two terms and thus controls a trade-off between the memorization of training examples and generalization to new instances.

The SVM algorithm is capable of handling extremely numerous and sparse features, thus allowing us to exploit a wide local context surrounding the cysteine under investigation. In particular, we provided information in the form of a symmetric window of $2k+1$ residues, centered around the target cysteine, with k varying from 1 to 25. In order to include evolutionary information, we coded each element of the window by its multiple alignment profile computed with *psiblast* (Altschul et al., 1997).

Preliminary model selection experiments were conducted in order to choose the appropriate kernel, together with its hyperparameters. In subsequent experiments we employed third degree polynomial kernels, with offset equal to one, fixed regularization parameter given by the inverse of the average of $K(x, x)$ with respect to the training set, and distinct penalties (Joachims, 1998) for errors on positive or negative examples, in order to rebalance the different proportion of examples in the two classes (see table 1). Similarity between examples $\boldsymbol{x}_i$ and $\boldsymbol{x}_j$ is therefore computed as

$$K(\boldsymbol{x}_i, \boldsymbol{x}_j) = (\boldsymbol{x}_i^T \boldsymbol{x}_j + 1)^3. \tag{3}$$

In order to include information about similarity between different residues, we also implemented a new kernel in which the dot product between $\boldsymbol{x}_i$ and $\boldsymbol{x}_j$ is mediated by a substitution matrix M:

$$K(\boldsymbol{x}_i, \boldsymbol{x}_j) = (\boldsymbol{x}_i^T M \boldsymbol{x}_j + 1)^3. \tag{4}$$

In order for equation (4) to be a valid kernel, matrix M has to be symmetric positive definite (Schölkopf and Smola, 2002). We tried the McLachlan aminoacid similarity matrix (McLachlan, 1972), which already satisfies such condition, and the Blosum62 (Henikoff and Henikoff, 1992) substitution matrix, that turned out to be positive definite after normalizing each element as $(M_{rc} - min)/(max - min)$ where max and min are over the entire matrix. A similar approach (Guermeur et al., 2004) was recently applied to secondary structure prediction.

3 Results and discussion

Test performances were calculated by three fold *cross validation*: proteins were divided in three groups, mantaining in each group approximately the same distribution of disulfide bridges and different kinds of metal binding sites.

The confusion matrix for PROSITE induced rules is shown in table 2 . It must be observed that the accuracy in table 2 is an optimistic upper bound of the true predictive power of this method with respect to future sequences. This is because PROSITE patterns have been designed to minimize the number of false hits and missed hits by actually inspecting the available sequence databases.

Results for the polynomial kernel are reported in figure 1. Train and test accuracies are plotted for growing size of the context window, with error bars for 95% confidence intervals, together to the fraction of support vectors over the train examples in the learned models, which is a rough indicator of the complexity of the learned models. The most evident improvement in test accuracy is obtained for a window of size k=3, and corresponds to the global minimum in the model complexity curve with about 56% of training examples as support vectors. Detailed results for such window are reported in table 3, showing they are obtained for an approximate break-even point in the precision recall curve. A deeper analysis of individual predictions showed that the vast majority of predictions were driven by the presence of a well conserved *CXXC* pattern, taken as the indicator of a metal binding. This explains the high rate of false positives compared to the total number of positive examples, being most of them cysteines containing the pattern but involved in disulfide bridges, while most of the false negatives are metal bindings missing it. The learned pattern is actually very common for most bindings involving iron-sulfur, iron-nickel and heme groups, and these kinds of metal binding are actually predicted with the highest recall.

The best accuracy is obtained for a window of size k=17, corresponding to about 87% of examples as support vectors. Detailed results are reported in tables 4 and 5, showing a strong reduction of false positives at the cost of a slight increase in the number of metal bindings predicted as disulfide bridges. Sequence logos (Schneider and Stephens, 1990) for cysteine context in the case of metal bindings (figure 2(upper)) show a well conserved *CXXCXXC* pattern, which is common in 4FE4S clusters, and the *CXXCH* pattern typical of heme groups, but also the presence of *CG* patterns in positions as distant as nine residues from the target cysteine. Disulfide bridge contexts are much more uniform (see figure 2(lower)), but show a strong tendency for polar aminos, especially glycine, cysteine and serine all along the window. The model seems capable of exploiting very distant information, and it discovers almost all rules induced by PROSITE patterns (see table 2), as only 13 over 202 metal bindings are lost, while it also corrects 8 over 15 false metal bindings. Moreover, the SVM is capable of discovering metal bindings sites where no pattern is available. In order to get some insights on the reasons for these predictions, we collected all the MBS that do not contain any pattern, and divided them into examples actually predicted as MBS by the SVM (true positives) and examples wrongly predicted as DB (false negatives). Figures 3(upper) and 3(lower) represent sequence logos for true positives and false negatives respectively, where the logos are computed using the average of the PSI-BLAST profiles of all the examples. Part of the correct predictions could be explained by the ability of the SVM to actually recover continuous-valued patterns in the profiles. We conjecture that in some other cases the predictor could have discovered potential consensus patterns that are still not known.

Reported results are quite robust with respect to model regularization, controlled by the cost parameter "C" in SVMs. Figure 4 shows a test accuracy maximization obtained by varying the regularization parameter: accuracies remain mostly within the confidence interval from the maximum. Table 6 shows test accuracies for different rejection rates, when predictions are to be made only if they are over a certain confidence. A rejection of 15% of both positive and negative test examples results in about 94% test accuracy, and predictions on disulfide bridges tend to be much more confident than those on metal bindings, having a higher threshold for equal rejection rate. Furthermore, metal bindings are rejected more frequently with respect to their total number in the test set. A finer analysis shows that rejected metal bindings are mostly those for which the model has low recall (see table 5), such as 3FE4S, iron, mercury and zinc, while 4FE4S, heme and nickel are seldom rejected. Figures 5(left) and 5(right) show precision/recall curves for disulfide bridges and metal bindings respectively, for different rejection rates. The former tends slightly towards the optimal curve at growing rejection rates, while the latter has a complementary behaviour with respect to the break-even point: at higher precisions growing rejection rates result in better performance, while at lower precisions preformance for growing rejection rates is affected by the greater quantity of metal bindings rejected with respect to disulfide bridges.

Figure 6(a) shows results for growing size of the context window, for a third degree polynomial kernel with McLachlan similarity matrix (eq. 4). While train and test accuracies are similar to those obtained without the similarity matrix (figure 1), the corresponding models have less support vectors, with reductions up to 11% of the training set. This behaviour is even more evident for the Blosum62 substitution matrix (figure 6(b)) where a slight decrease in test accuracy, still within the confidence interval, corresponds to a reduction up to 30% of the training set. Note that the fraction of support vectors

over training examples is a loose upper bound on the leave one out error (Vapnik, 1995), which is an almost unbiased estimate of the true generalization error of the learning algorithm (see for example (Elisseeff and Pontil, 2003)). These kernels are able to better exploit information on residue similarity, thus obtaining similar performances with simpler models. Moreover, the precision/recall rate of the kernel with the blosum62 matrix is much more balanced with respect to the other two, meaning that it suffers less from the unbalancing in the training set.

4 Conclusions

We have proposed learning algorithms for predicting the type of binding in which non-free cysteines are involved. The experimental results indicate that learning from multiple alignment profiles data outperforms even non-trivial approaches based on pattern matching, suggesting that relevant information is contained not only in the residues flanking the cysteine but also in their conservation. In some cases the learning algorithm could be actually exploiting in a probabilistic way patterns that are not yet listed in PROSITE, although detecting them with few data points is difficult. In addition, we found that using residue similarity matrices effectively reduces the complexity of the model measured by the number of support vectors, which is also an indication of the expected generalization error. We expect that similar kernel functions could be also useful for other predictive tasks both in 1D (e.g. solvent accessibility) and in 2D (e.g. contact maps), especially if task-dependent similarity matrices could be devised.

5 Acknowledgements

We thank B. Rost and M. Punta for providing part of the data used in the experiments and S. Ciofi-Baffoni for useful discussions. This work is partially supported by Italian MIUR grant # 2002093941.

References

Altschul, S. F., Madden, T. L., Schaffer, A. A., Zhang, J., Zhang, Z., Miller, W., and Lipman, D. J. (1997). Gapped blast and psi-blast: a new generation of protein database search programs. *Nucleic Acids Res.*, 25(17):3389–3402.

Balatri, E., Banci, L., Bertini, I., Cantini, F., and Ciofi-Baffoni, S. (2003). Solution structure of sco1: a thioredoxin-like protein involved in cytochrome c oxidase assembly. *Structure*, 11(11):1431–1443.

Berman, H. M., Westbrook, J., Feng, Z., Gilliland, G., Bhat, T. N., Weissig, H., Shindyalov, I. N., and Bourne, P. E. (2000). The protein data bank. *Nucleic Acids Res.*, 28:235–242.

Boeckmann, B., Bairoch, A., Apweiler, R., Blatter, M. C., Estreicher, A., Gasteiger, E., Martin, M. J., Michoud, K., O'Donovan, C., Phan, I., Pilbout, S., and Schneider, M. (2003). The swiss-prot protein knowledgebase and its supplement trembl in 2003. *Nucleic Acids Res.*, 31(1):365–370.

Chinenov, Y. (2000). Cytochrome c oxidase assembly factors with a thioredoxin fold are conserved among prokaryotes and eukaryotes. *J. Mol. Med.*, pages 239–242.

Cortes, C. and Vapnik, V. (1995). Support vector networks. *Machine Learning*, 20:1–25.

Cristianini, N. and Shawe-Taylor, J. (2000). *An Introduction to Support Vector Machines*. Cambridge University Press.

Elisseeff, A. and Pontil, M. (2003). Leave-one-out error and stability of learning algorithms with applications. In Suykens, J., Horvath, G., Basu, S., Micchelli, C., and Vandewalle, J., editors, *Advances in Learning Theory: Methods, Models and Applications*, volume 190 of *NATO Science Series III: Computer & Systems Sciences*, pages 111–130. IOS Press Amsterdam.

Falquet, L., Pagni, M., Bucher, P., Hulo, N., Sigrist, C., Hofmann, K., and Bairoch, A. (2002). The PROSITE database, its status in 2002. *Nucleic Acids Res.*, 30(1):235–238.

Fiser, A. and Simon, I. (2000). Predicting the oxidation state of cysteines by multiple sequence alignment. *Bioinformatics*, 16(3):251–256.

Gattiker, A., Gasteiger, E., and Bairoch, A. (2002). ScanProsite: a reference implementation of a PROSITE scanning tool. *Applied Bioinformatics*, 1:107–108.

Guermeur, Y., Lifchitz, A., and Vert, R. (2004). A kernel for protein secondary structure prediction. In Schölkopf, B., Tsuda, K., and Vert, J. P., editors, *Kernel Methods in Computational Biology*. The MIT Press, Cambridge, MA. In press.

Heaton, D., George, G., Garrison, G., and Winge, D. (2001). The mitochondrial copper metallochaperone cox17 exists as an oligomeric, polycopper complex. *Biochemistry*, 40(3):743–751.

Henikoff, S. and Henikoff, J. G. (1992). Amino acids substitution matrices from protein blocks. *Proc. Natl. Acad. Sci. U.S.A.*, 89(22):10915–10919.

Joachims, T. (1998). Making large-scale SVM learning practical. In Schölkopf, B., Burges, C., and Smola, A., editors, *Advances in Kernel Methods – Support Vector Learning*, chapter 11, pages 169–185. MIT Press.

Martelli, P. L., Fariselli, P., Malaguti, L., and Casadio, R. (2002). Prediction of the disulfide bonding state of cysteines in proteins with hidden neural networks. *Protein Eng.*, 15:951–953.

Mathews, F. (1985). The structure, function and evolution of cytochromes. *Prog. Biophys. Mol. Biol.*, 45(1):1–56.

McLachlan, A. (1972). Repeating sequences and gene duplication in proteins. *J Mol. Biol.*, 64:417–437.

Mika, S. and Rost, B. (2003). Uniqueprot: creating sequence-unique protein data sets. *Nucleic Acids Res.*, 31(13):3789–3791.

Mucchielli-Giorgi, M., Hazout, S., and Tuffèry, P. (2002). Predicting the disulfide bonding state of cysteines using protein descriptors. *Proteins*, 46:243–249.

Otaka, E. and Ooi, T. (1987). Examination of protein sequence homologies: Iv. twenty-seven bacterial ferredoxins. *J. Mol. Evol.*, 26(3):257–67.

Quinlan, J. (1986). Inductive learning of decision trees. *Machine Learning*, 1:81–106.

Quinlan, J. (1993). *C4.5: Programs for machine learning*. Morgan Kaufmann Publishers.

Schneider, T. D. and Stephens, R. M. (1990). Sequence logos: A new way to display consensus sequences. *Nucleic Acids Res.*, 18:6097–6100.

Schölkopf, B. and Smola, A. (2002). *Learning with Kernels*. The MIT Press, Cambridge, MA.

Vapnik, V. N. (1995). *The Nature of Statistical Learning Theory*. Springer, New York.

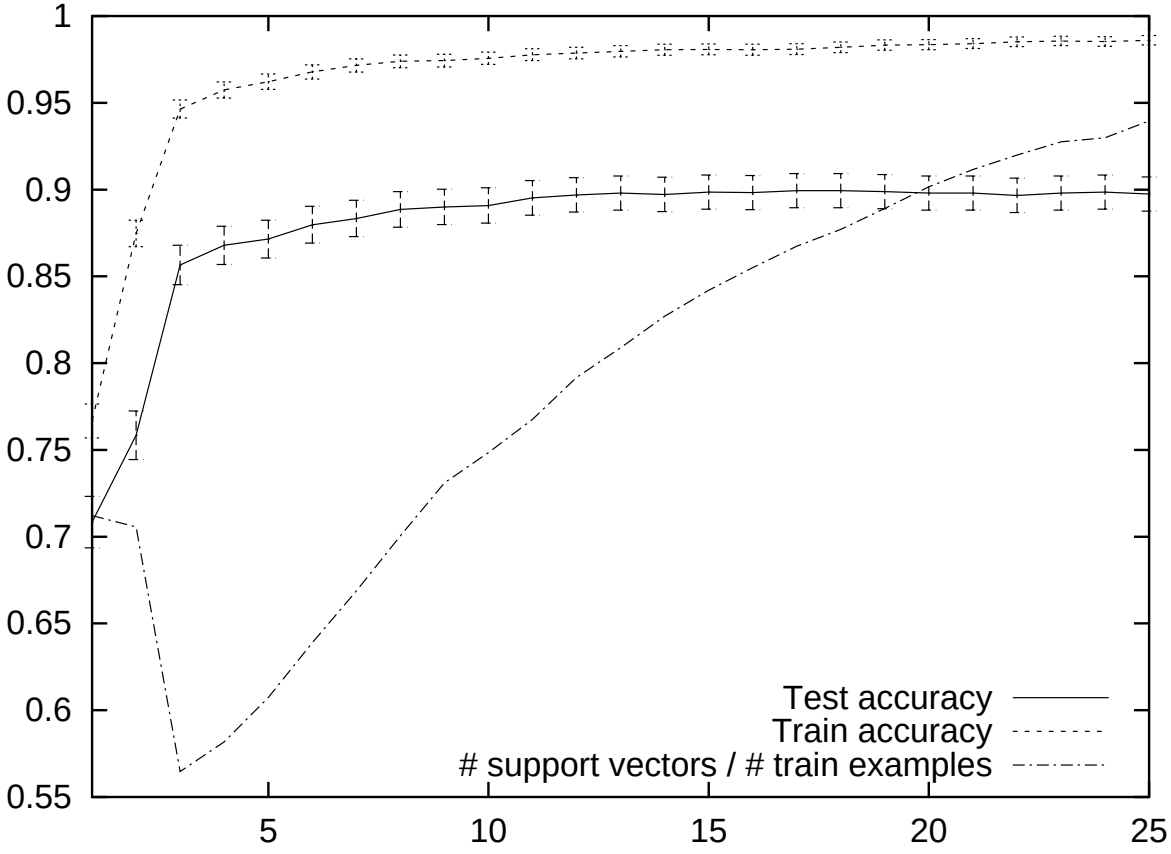
1
0.95
0.9
0.85
0.8
0.75
0.7
0.65
0.6
0.55
5
10
15
20
25
Test accuracy
Train accuracy
support vectors / # train examples

Figure 1:

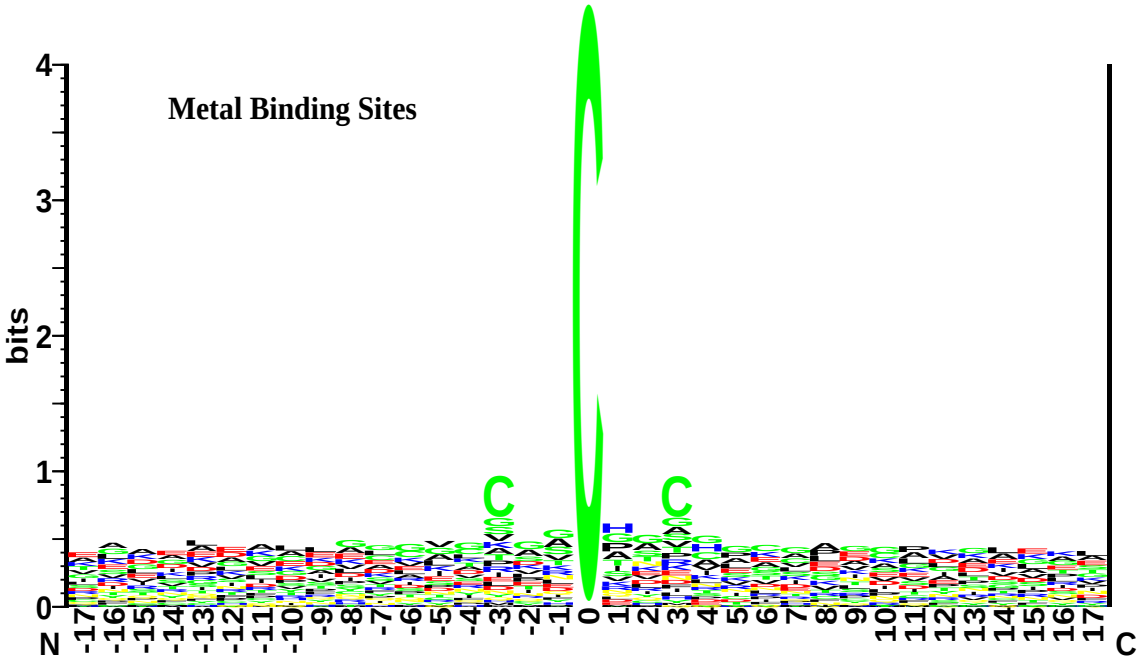

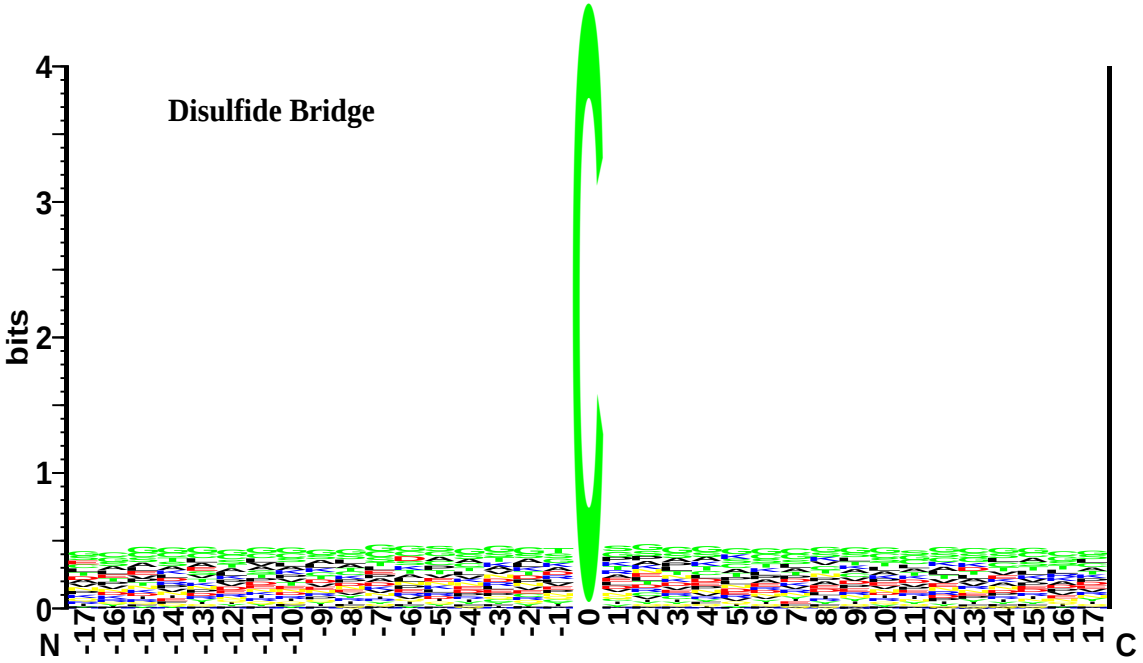

Figure 2:

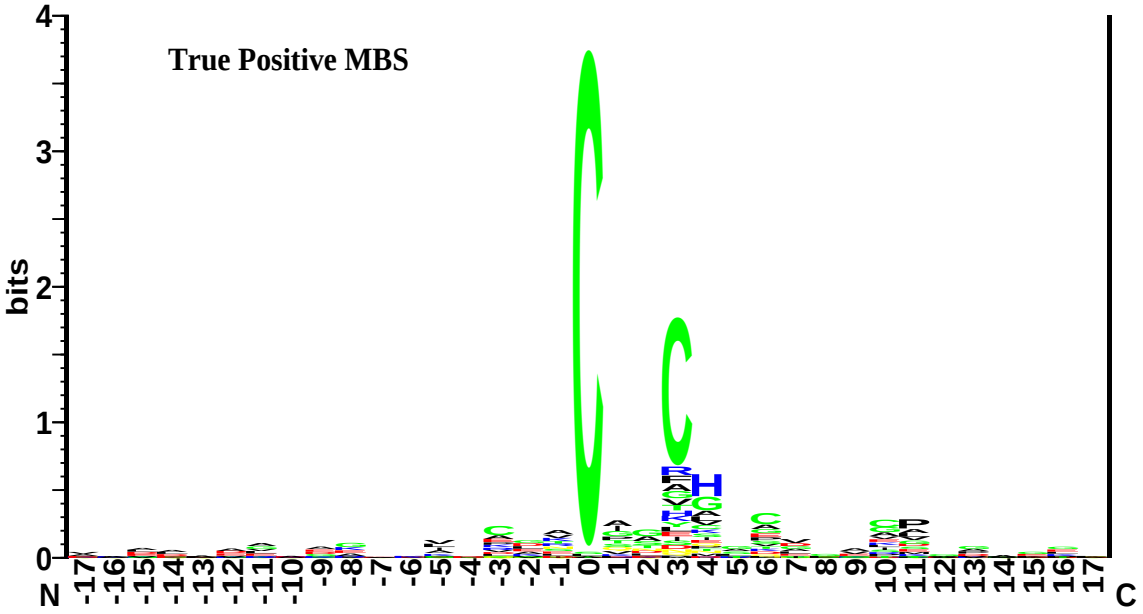
True Positive MBS
bits
4
3
2
1
0
N
C
-17 -16 -15 -14 -13 -12 -11 -10 -9 -8 -7 -6 -5 -4 -3 -2 -1 0 1 2 3 4 5 6 7 8 9 10 11 12 13 14 15 16 17

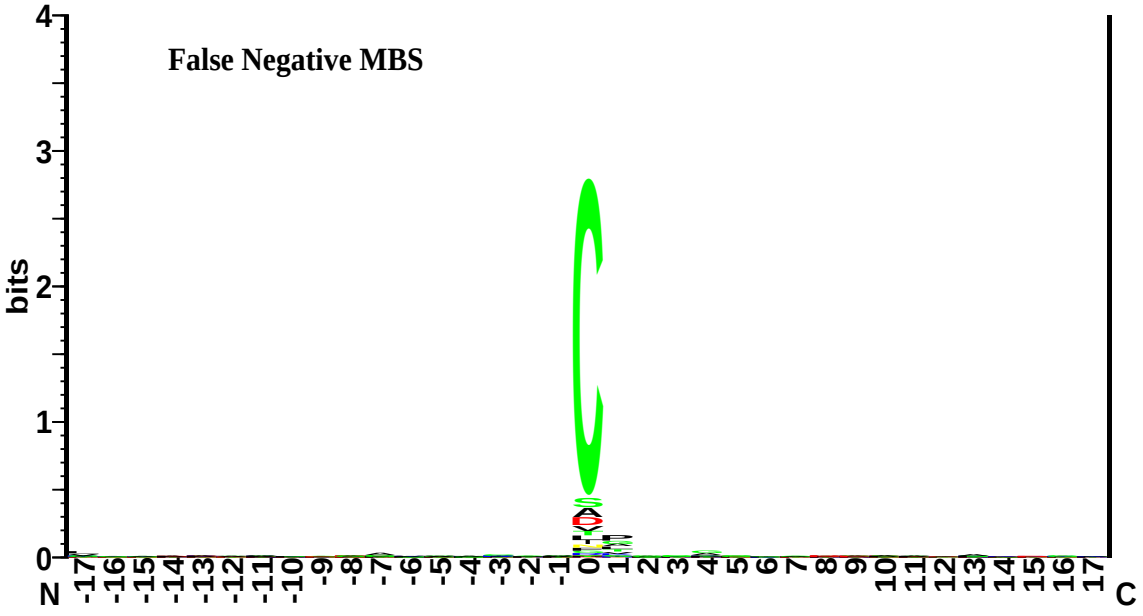
False Negative MBS
bits
4
3
2
1
0
N
C
-17 -16 -15 -14 -13 -12 -11 -10 -9 -8 -7 -6 -5 -4 -3 -2 -1 0 1 2 3 4 5 6 7 8 9 10 11 12 13 14 15 16 17

Figure 3:

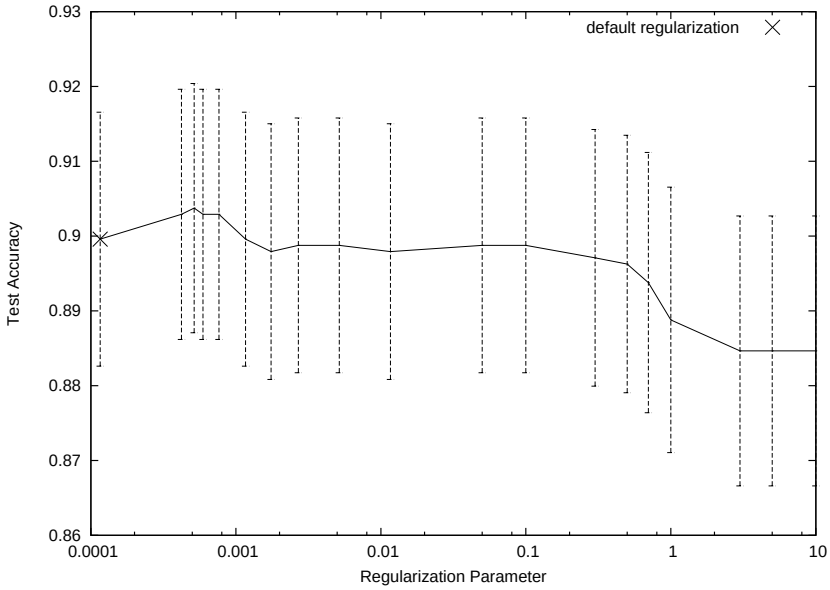

Figure 4:

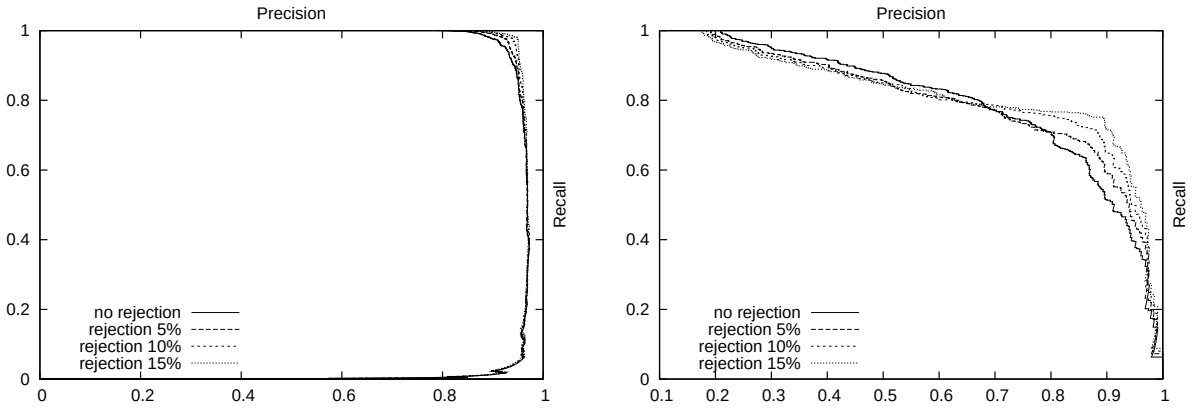

Figure 5:

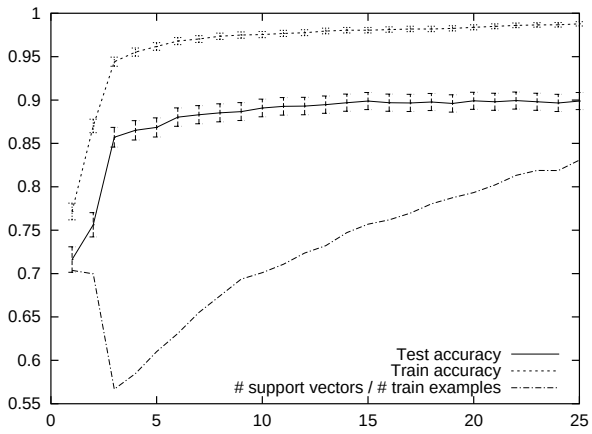

(a) Polynomial Kernel with McLachlan Matrix

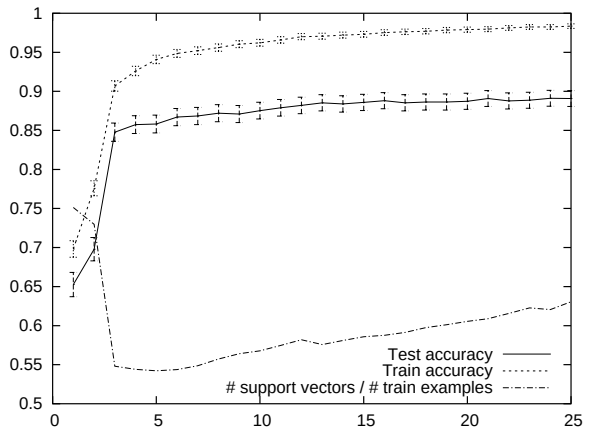

(b) Polynomial Kernel with Blosum62 Matrix

Figure 6:

Figure 1: Disulfide bridge vs metal binding prediction by SVMs with 3^{rd} degree polynomial kernel. Test and train accuracies with 95% confidence intervals are plotted, together to the fraction of support vectors over the number of training examples, for growing sizes of the window of $2k+1$ residues profiles around the target cysteine, with k going from 1 to 25. Results are averaged over a three fold cross validation procedure.

Figure 2: Sequence logos (Schneider and Stephens, 1990) of context of cysteines involved in metal bindings (upper) and disulfide bridges (lower) respectively, with a window of 17 residues on each side of the bond cysteine. Hydrophobic residues are shown in black, positively charged residues are blue and negatively charged are red, while uncharged polar residues are green.

Figure 3: Sequence logos (Schneider and Stephens, 1990) of 17 aminos context of cysteines that don't match any PROSITE pattern, and are either truly predicted as MBS (upper) or mistakenly predicted as DB (lower) by an SVMs with 3^{rd} degree polynomial kernel. Hydrophobic residues are shown in black, positively charged residues are blue and negatively charged are red, while uncharged polar residues are green.

Figure 4: Disulfide bridge vs metal binding prediction by 3^{rd} degree polynomial kernel SVMs. Window of 17 residues profiles on both sides of the target cysteine. Test accuracies with 95% confidence intervals are plotted versus "C" regularization parameter of SVMs. Default regularization is computed as the inverse of the average of $K(x, x)$ with respect to the training set.

Figure 5: Disulfide bridge vs metal binding prediction by 3^{rd} degree polynomial kernel SVMs. Window of 17 residues profiles on both sides of the target cysteine. Precision/recall curves over the test set for different rejection rates for disulfide bridge (left) and metal binding (right) prediction.

Figure 6: Disulfide bridge vs metal binding prediction by SVMs with 3^{rd} degree polynomial kernel with McLachlan (a) or Blosum62 (b) similarity matrix. Test and train accuracies with 95% confidence intervals are plotted, together to the fraction of support vectors over the number of training examples, for growing sizes of the window of $2k+1$ residues profiles around the target cysteine, with k going from 1 to 25. Results are averaged over a three fold cross validation procedure.

	# Sequences	# Cysteines
Disulfide Bridges	529	2860
Metal Bindings	202	758

Table 1: Non homologous sequences obtained by running *uniqueprot* (Mika and Rost, 2003) with hssp distance set to zero. Sequences containing disulfide bridges were obtained from resolved proteins in PDB (Berman et al., 2000), while those with metal bindings were recovered from SWISSPROT version 41.23 (Boeckmann et al., 2003) by keyword matching.

	Precision (%)	Recall (%)	Bridge	Metal	
Bridge	84	99	2845	15	True
Metal	93	27	556	202	
Accuracy	84.2		Predicted		

Table 2: Disulfide bridge vs metal binding prediction by decision rules learned by c4.5 from patterns extracted from PROSITE. Precision and recall for both classes, confusion matrix and overall accuracy.

	Precision (%)	Recall (%)	Bridge	Metal	
Bridge	91	90	2588	272	True
Metal	65	67	247	511	
Accuracy	86		Predicted		

Table 3: Disulfide bridge vs metal binding prediction by 3^{rd} degree polynomial kernel SVMs. Window of 3 residues profiles on both sides of the target cysteine. Precision and recall for both classes, confusion matrix and overall accuracy.

	Precision (%)	Recall (%)	Bridge	Metal	
Bridge	91	97	2788	72	True
Metal	87	61	292	466	
Accuracy	90		Predicted		

Table 4: Disulfide bridge vs metal binding prediction by 3^{rd} degree polynomial kernel SVMs. Window of 17 residues profiles on both sides of the target cysteine. Precision and recall for both classes, confusion matrix and overall accuracy.

Ligand	**# examples**	**Recall** (%)
Cysteine	2860	97.5
Metal	758	61.4
4FE4S	250	71.6
Zinc	156	38.5
Heme	139	87.8
2FE2S	91	58.2
Copper	50	38.0
Iron	26	42.3
3FE4S	25	48.0
Nickel	13	76.9
Mercury	7	00.0
Manganese	1	00.0

Table 5: Disulfide bridge vs metal binding prediction by 3^{rd} degree polynomial kernel SVMs. Window of 17 residues profiles on both sides of the target cysteine. Recall and number of examples for cysteine (disulfide bridge) or metal ligand, and details for different kinds of metal binding.

	Threshold			Bridge		Metal		Rejected (%)	
Rejection (%)	Bridge	Metal	Acc	Pre	Rec	Pre	Rec	Bridge	Metal
00	0	0	89.9	90.5	97.5	86.6	61.5	0.0	0.0
05	0.20845	0.0470436	91.8	92.7	97.6	86.9	67.4	02.8	12.9
10	0.340927	0.113824	93.0	93.8	97.9	88.5	71.5	07.1	20.8
15	0.436391	0.159688	94.0	94.8	98.1	89.3	75.2	11.4	28.2
20	0.506477	0.225416	94.4	95.2	98.2	90.3	76.6	16.5	33.0
25	0.56122	0.267722	95.2	95.9	98.4	91.1	79.5	21.3	38.8
30	0.609002	0.337221	95.7	96.1	98.8	93.4	80.8	26.6	42.3

Table 6: Disulfide bridge vs metal binding prediction by 3^{rd} degree polynomial kernel SVMs. Window of 17 residues profiles on both sides of the target cysteine. Performances for different rejection rates, where rejection percentage is computed separately for examples predicted as bridge or metal, in order to consider the unbalanced distribution of examples between the two classes (i.e. 5% rejection rate indicates that 5% of examples predicted as bridges are to be rejected, as well as 5% of examples predicted as metal). Reported results include rejection thresholds, accuracies, precision and recall, and percentage of rejected examples belonging to each of the two classes.